American Mineralogist
Vol. 57, pp. 1692–1710 (1972)

INTERPRETATION OF THE SPIN-ALLOWED BANDS OF Fe^{2+} IN SILICATE GARNETS

WILLIAM B. WHITE AND RAYMOND K. MOORE,[1]

Materials Research Laboratory and Department of Geosciences,
The Pennsylvania State University,
University Park, Pennsylvania 16802

ABSTRACT

The three intense near–infrared bands of Fe^{2+} in silicate garnets at approximately 4500, 6000, and 7800 cm^{-1} are assigned to transitions from the d_{z^2} orbital ground state to the $d_{x^2-y^2}$, d_{yz}, and d_{xz} orbitals respectively. The temperature dependence of the band intensities implies that the transitions are vibronically coupled by phonons with frequencies of 835 and 695 cm^{-1}. The mean frequency is a measure of Dq for the 8–fold site and decreases with increasing mean X–O distance. The frequency difference between the d_{xz} and d_{yz} orbitals is shown to be a measure of the distortion of the 8–fold site. Revised crystal field stabilization energies for Fe^{2+} in garnet are 10.26 to 10.72 kcal/mole.

INTRODUCTION

The electronic spectra of transition metal ions in garnets have been studied by many workers (Clark, 1957; Manning, 1967a, 1967b, 1969; Burns, 1969, 1970; Moore and White, 1972). The garnets exhibit some of the most complex spectra of any known silicate minerals. Previous work has established the relationship of the spectral bands to energy levels of Fe^{2+}, Fe^{3+}, Mn^{2+}, Cr^{3+}, and V^{3+} on mainly the 6–fold and 8–fold sites of the garnet structure. Most important is the spectrum of Fe^{2+}. It is generally agreed that Fe^{2+} is responsible for a group of three strong bands in the near infrared due to spin–allowed transitions and for a number of weak sharp bands in the visible due to spin–forbidden transitions.

The present paper is concerned only with the three spin–allowed bands of Fe^{2+} on the 8–fold site in garnet. The object is to provide a detailed assignment for these bands in terms of the arrangement of the orbitals in the site and to relate the frequencies of these bands to the crystal chemistry of the garnets. Crystal chemical and crystallographic data are available in an extensive set of structural refinements (Novak and Gibbs, 1971) and in a review article (Geller, 1967).

---

[1] Present address: Department of Natural Sciences, Radford College, Radford, Virginia.

EXPERIMENTAL

A suite of 13 garnets from ugrandite and pyralspite families were studied. Chemical analyses were reported in the first part of this study (Moore and White, 1972) and are not repeated here. Measured lattice parameters and calculated molecular proportions of the end members are listed in Table 1. All specimens were optically homogeneous single crystals. The crystals were sliced and ground to approximately 0.25 to 0.50 mm thickness. The samples were then polished to a glass finish on three-micron grit for optical absorption measurements.

The absorption spectra between 0.3 and 2.6 microns were collected on both the Beckman DK-2A and the Cary 14 spectrophotometers. The spectra run as a function of temperature were obtained using the Cary 14 with a cold cell and liquid nitrogen; and for high-temperature work a soldering gun variac combination was used with thermocouple measurement of the temperature. All variable temperature measurements were obtained in triplicate to insure constant temperature and accurate intensity variations.

OPTICAL SPECTRA

The three strong bands in the near infrared appear best in the spectra of the pyralspites. A typical spectrum is shown in Figure 1. All pyralspites examined show this group of three bands (labeled a, b, and c) in Figure 1 near 4300, 5900, and 7700 cm^{-1}. From their intensity and half width it seems safe to infer that these are spin-allowed transitions. Frequencies and intensities for all specimens are listed in Table 2.

The same bands appear in the spectra of grossularite but are of much lower intensity because of the low concentration of ferrous iron. Usually the weak a-band was not observed. Frequencies and intensities for the other two bands are listed in Table 2.

Manning (1967a) assigned this group of bands to Fe^{2+} on the 8-fold site. This assignment is substantiated by Figure 2 in which is plotted the absorbance of the band per unit thickness as a function of FeO content. The Beer's law plot shows that all three bands vary nearly linearly with increasing ferrous iron content. The scatter in the individual points may be due to inaccuracies in the chemical analysis for FeO, since the scatter is in the same direction for each band. Analysis for FeO in silicate garnets is difficult and Figure 2 suggests that a spectrophotometric analysis could be used to give better results.

No evidence was found for the 2900 cm^{-1} band reported by Clark (1957) in agreement with Manning's (1967a) observation. Calculations based on the assumption that the 2900 cm^{-1} band is due to Fe^{2+} (such as those of Bloomfield, Lawson and Rey, 1961) should be reexamined.

TABLE 1. LATTICE PARAMETER AND MOLECULAR PROPORTIONS FOR GARNET SPECIMENS

Sample	Lattice Parameter(Å)	Py	Al	Sp	Gr	An	Uv
Al-77	11.5019	18.0	77.0	---	4.6	0.4	---
Al-76	11.5127	8.0	76.0	3.6	13.0	---	---
Al-68	11.5292	22.6	67.8	5.0	3.3	1.3	---
Al-67*	11.5167	23.0	67.5	3.0	6.4	---	---
Al-51	11.5160	33.6	51.0	0.9	13.1	1.4	---
Py-71*	11.5302	71.4	16.0	0.9	3.4	1.0	7.3
Py-59*	11.5026	59.1	37.5	1.7	1.7	---	---
Sp-70	11.6116	6.8	22.4	70.0	---	0.8	---
Sp-53*	11.571	0.9	45.5	53.0	0.7	---	---
Gr-90	11.8478	---	3.2	0.6	89.9	6.4	
Gr-87	11.8412	---	6.0	0.6	87.3	6.4	
Gr-74	11.8512	0.5	4.7	2.6	73.6	18.4	

*Assumes all iron is one valency state, Fe^{++} in pyralspite and Fe^{+++} in ugrandites.

Agreement in frequency values of the band maximum with those reported by Manning (1967a) is good. The frequencies of this set of bands vary little with the pyralspite composition.

Molar extinction coefficients were calculated from the slopes of the lines in Figure 2 and are shown on the figure. These are based on $\epsilon = A/(tC)$, where C is the concentration of Fe^{2+} ions in moles per liter of garnet host. These are of the correct order of magnitude expected for *d–d* transitions.

The behavior of the a, b, and c bands with varying temperatures was measured. The results for specimen Al–77 are shown in Figure 1. At temperatures down to 78 K the main effect is a general lowering of intensity, a slight sharpening of the bands, and a mild frequency shift. No additional fine structure was observed. The frequency shifts are small and difficult to measure from these relatively broad bands. The frequency changes, related to the value at 78 K are shown in Figure 3. Of interest is the observation that the b– and c–bands increase in

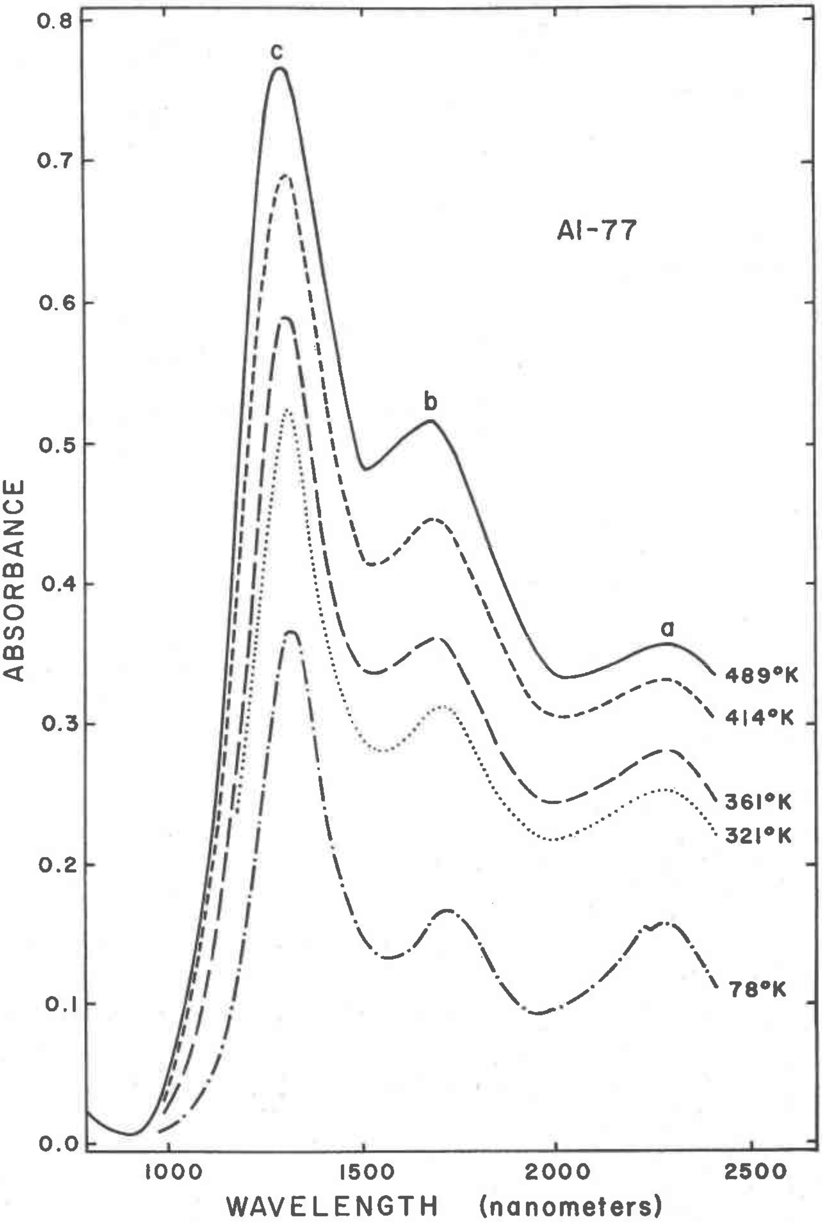

FIG. 1. Near infrared spectra of a pyralspite $Al_{0.77}Py_{0.18}Gr_{0.0046}An_{0.004}$ at various temperatures.

TABLE 2. FREQUENCIES OF THE SPIN-ALLOWED a, b, AND c BANDS IN THE SAMPLES STUDIED. ABSORBANCES/mm ARE PRESENTED IN PARENTHESES.

Sample	Band a	Band b	Band c
Al-77	4381(1.07)	5874(1.44)	7663(2.40)
Al-76	4303(1.17)	5868(1.44)	7633(2.48)
Al-68	4312(1.02)	5884(1.30)	7668(2.19)
Al-67	4348(0.90)	5917(1.12)	7657(1.99)
Al-51	4390(0.49)	6011(0.68)	7770(1.62)
Sp-70	4244(0.39)	5924(0.49)	7770(0.84)
Sp-53	4310(0.18)	5951(0.49)	7752(1.17)
Py-71	4651(0.10)	6211(0.22)	7888(0.42)
Py-59	4533(0.64)	6068(0.80)	7764(1.30)
Py-Cr(III)	4666(0.20)	6139(0.27)	7831(0.42)
Gr-87	--	5760(0.03)	8150(0.08)
Gr-74	--	5830(0.09)	8233(0.18)
Gr-90	--	5800(0.07)	8210(0.13)

frequency with decreasing temperature (the expected result from the stronger crystal field resulting from shortened metal–oxygen distances due to thermal contraction), but the a–band decreases in frequency with decreasing temperature.

INTERPRETATION OF THE SPECTRA

Assignments

The cubal coordination polyhedron based on a drawing by Prandl (1966) is shown in Figure 4. The distorted cube has site symmetry D_2. The labeling of the three 2–fold axes of D_2 is arbitrary in so far as the crystal is concerned but is not arbitrary if one wants to use the usual labeling for spectroscopic terms and the descent–of–symmetry tables, both of which assume particular conventions for labeling of the coordinate system. It should also be noted that these 2–fold axes are proper symmetry elements of the space group, *Ia3d*. They are not merely pseudo–symmetries of the coordination polyhedron. One 2–fold axis is unique in that it lies in the center of a face of the

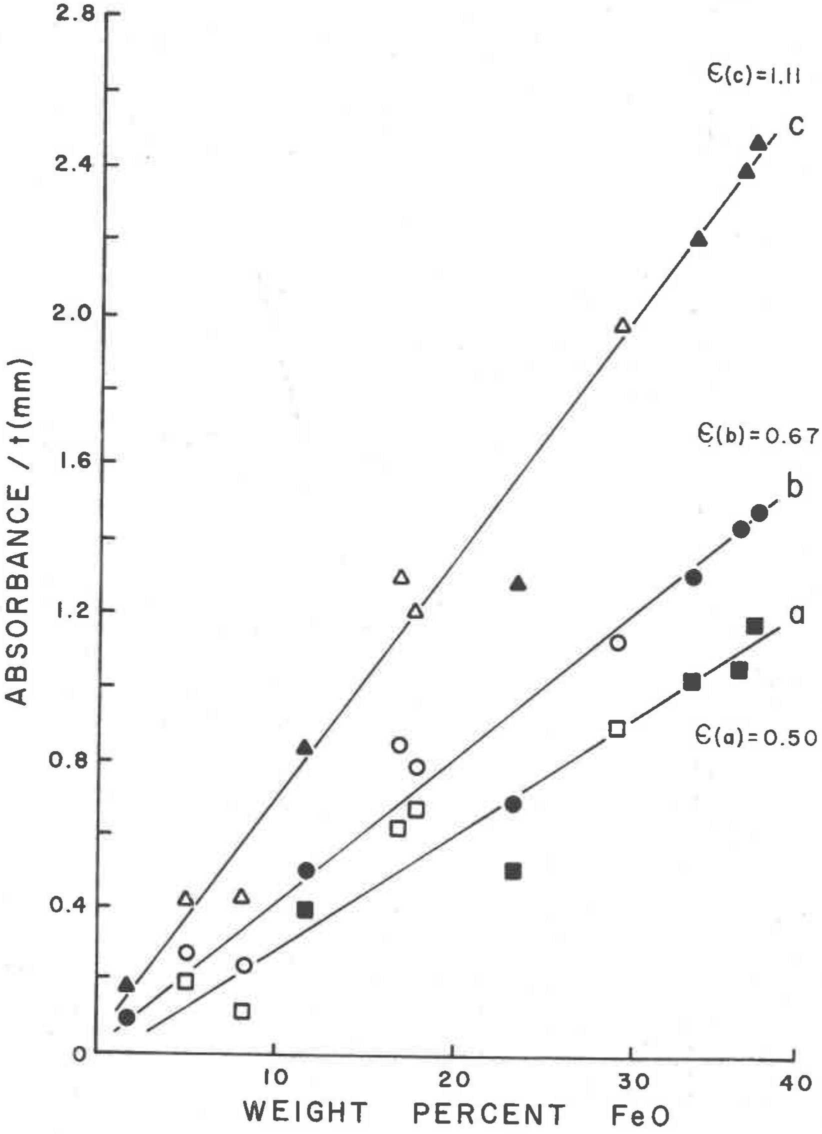

FIG. 2. Beer's Law plots for the spin-allowed bands of the pyralspites. Solid points represent samples for which FeO was determined by chemical analysis. Open points represent samples for which total iron was calculated as FeO.

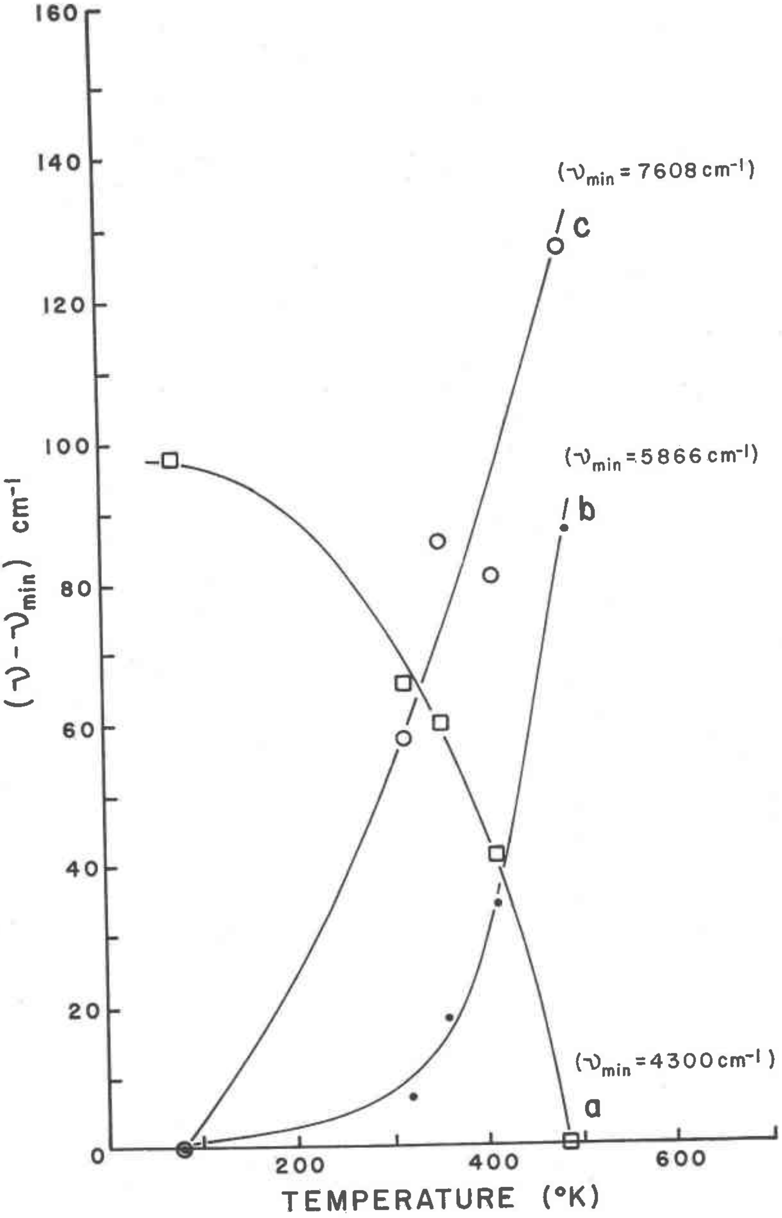

FIG. 3. Frequency shift in near-infrared spin-allowed bands as a function of temperature.

distorted cube. The other two bisect the cube edges and lie in a plane perpendicular to the unique axis. There are two ways in which the sub-group D_2 may be constructed from the elements of the parent cubic group, O_h. The construction appropriate to garnet requires one C_2 axis to be selected from the class $3C_2$ which are coincident with the 4-fold axes of the cube, and two C_2 axes to be selected from the class $6C_2$ which are the diagonal axes bisecting the cube edges. These requirements, and the proper alignment of the coordinate systems, are met if the unique axis centered on the polyhedron face is labeled $C_2(z)$ as shown in Figure 4.

Divalent iron has a single quintet ground state which is split by an octahedral crystal field into a lower $^5T_{2g}$ level and an upper ^5E_g level with an energy separation of about 10,000 cm^{-1}. See Jones (1967) for typical values in crystalline hosts.

Assuming that the oxygens behave as point electrostatic charges, the splitting of the quintet term in a cubal field is $-8/9$ of the octahedral value if the interatomic distances remain constant (Fig. 5).

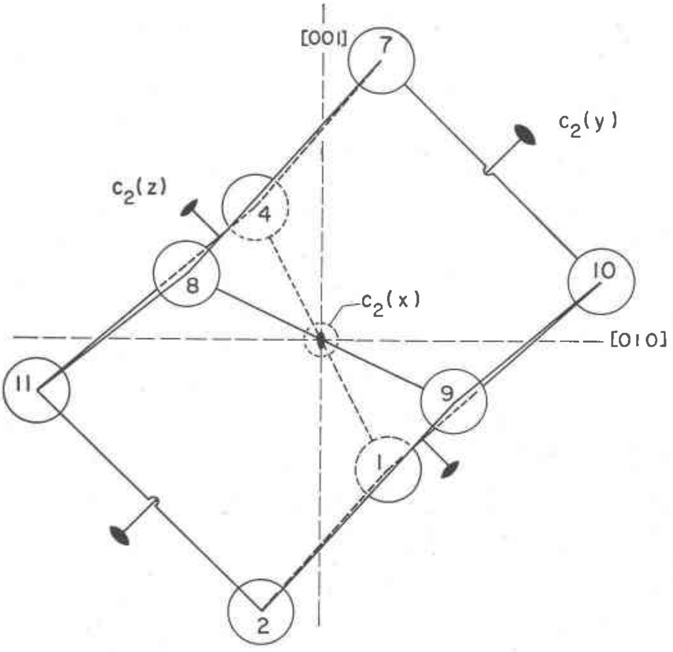

FIG. 4. The cubal site in garnet showing the relation of the site symmetry axes to the crystallographic axes. Oxygens numbered according to convention of Prandl (1966).

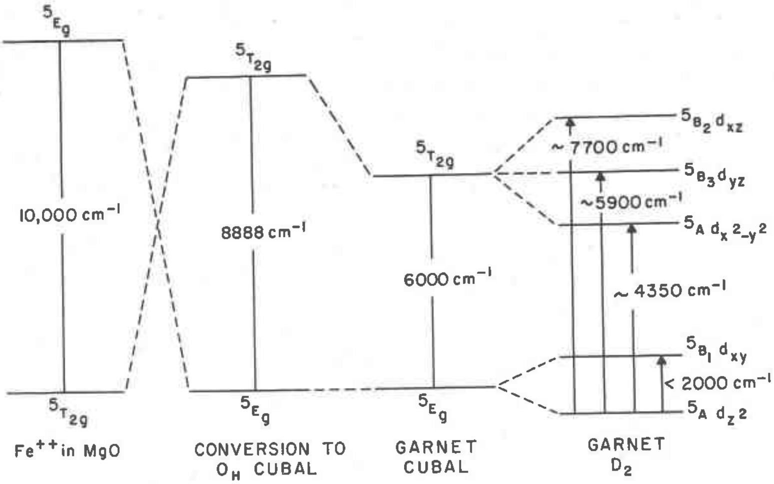

FIG. 5. Energy level scheme for the splitting of the Fe^{2+} quintet term in various fields.

Using the spectrum of Fe^{2+} in MgO as a reference point and remembering that the crystal field varies with the inverse fifth power of the interatomic distance, an estimation of the average energy level separation in garnet is given by

$$10{,}000 \times 8/9 \times \left(\frac{2.27}{2.10}\right)^{5} \cong 6{,}000 \text{ cm}^{-1}.$$

The interatomic distances are those in MgO and the average X–O distance in pyrope (Gibbs and Smith, 1965). The calculated splitting is almost exactly the average frequency of the three spin–allowed bands.

The distortion of the cubal site to a triangular dodecahedron lifts the degeneracy of the cubic field levels. The labeling of the resultant states is obtained from the descent–of–symmetry tables of Wilson, Decius, and Cross (1955, p. 340).

$$T_{2g} \rightarrow A + B_2 + B_3$$

$$E_g \rightarrow A + B_1.$$

The center–of–gravity rule for orbital splitting is expected to hold if the orbitals do not mix. Since there are no other quintet levels and since only the A terms of the excited and ground states could interact, one might expect the T_{2g} level to split into three components whose average is close to the expected energy for the cubic field. What is in fact observed is a separation into terms spaced about 1700 cm^{-1} apart. The middle band at 5900 cm^{-1} is very close to the expected average value of 6,000 cm^{-1}.

The analysis given above is probably not as elegant as the numbers indicate, because it ignores the splitting of the ground state. If this splitting were large, the transitions would increase in energy because of the lowering of the new ground state. No band which might correspond to the $A \rightarrow B_1$ transition between the two levels derived from E_g was observed in the range of 1500—4500 cm^{-1}. It was therefore concluded that the ground state splitting was small, and it is so indicated in Figure 5.

The energy level diagram of Figure 5 differs from that published by Burns (1970). Burns apparently accepted Clark's (1957) report of a band at 2900 cm^{-1} and assigned it to the transition between the two components of the E_g level. Burns likewise finds only 4520 cm^{-1} as the separation of the centers of gravity of the T_{2g} and E_g levels. His value seems much too low to be consistent with the average size of the site.

The rigorous group theoretical analysis gives the degree of splitting and the labeling of the resultant states but says nothing about the energies of these states. Relative energies can be obtained by an actual solution of the secular equation in the manner of Garner and Mabbs (1970) or Randić (1962). However, one may obtain an empirical fit of the relative energies by an examination of the way in which the orbitals fit into the coordination polyhedron. Figure 6 shows an alternate view of the 8-fold site (based on Gibbs and Smith, 1965) drawn as an undistorted cube and giving the bond lengths of pyrope. The axes follow the convention established in Figure 4. The orbitals have been inserted in their proper location in the boxes to conform to the axis designation. The transformation properties of the orbitals in D_2 symmetry are;

$$dx^2, dy^2, dz^2 \rightarrow A$$

$$dxy \rightarrow B_1$$

$$dxz \rightarrow B_2$$

$$dyz \rightarrow B_3$$

The orbital lobes of d_{z^2} and dxy point to the centers of cube faces and will suffer the least repulsion by the O^{2-} charges. These should belong to the components of the cube ground state and indeed $E_g \rightarrow A + B_1$ under this axis arrangement. Deciding which orbital has the lower energy and thus is the ground state in the distorted cube is more difficult.

Examination of the lengths of the cell edges in Figure 6b suggests that d_{xy} will sense a slightly stronger field than d_{z^2} because of the contraction of the cube along the 2.496Å edge. d_{z^2} will then be the ground state, but the actual energy separation will be small, in agreement with the lack of any observed transition above 1500 cm^{-1}.

The remaining three orbitals are the components of the T_{2g} excited state. The lobes of $d_{x^2-y^2}$ point to the cube edges along the x and y axes. $d_{x^2-y^2}$ should interact more weakly with the ligands than either dxz or dyz which point toward the ligands along the cube diagonals. Therefore, $d_{x^2-y^2}$ should have the lowest energy of the three. This assignment is in agreement with the qualitatively different behavior of the a–band as a function of temperature. Examination of Figure 6d shows that the

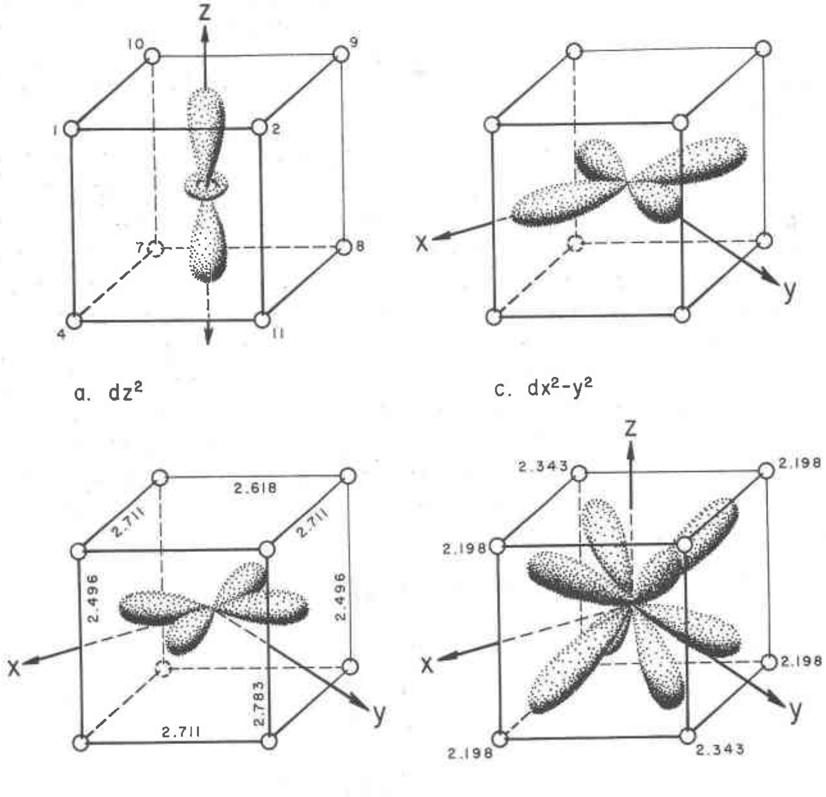

a. dz²

c. dx²-y²

b. dxy

d. dxz and dyz

FIG. 6. Schematic views of the cubal site showing the location of five *d*–orbitals in the polyhedron. Bond and edge lengths are appropriate for pyrope (after Gibbs and Smith, 1965).

four lobes of d_{yz} are oriented along the four short (2.198Å) Fe–O bonds, while the d_{xz} lobes lie along the long (2.243Å) bonds. d_{yz} should experience the strongest interaction and thus is assigned to the highest energy, while d_{xz} is assigned to the intermediate one. These assignments are summarized in Figure 5.

It should be noted that the distortion of the cube site also affects the geometry of the orbitals. The four lobes of d_{xz} (and d_{yz}) transform into each other by the operations of the 2–fold symmetry axes so these orbitals retain their symmetrical shape. The same is not true of d_{xy} and $d_{x^2-y^2}$. The two ends of the x–axis lobe of $d_{x^2-y^2}$ (and likewise of the y–axis lobe) are interchanged by $C_2(z)$ but the x–axis lobes and y–axis lobes are not related to each other by a symmetry operation. The rigorous linear combination which generates $d_{x^2-y^2}$ in a cubic site is broken and the two pairs of lobes need not have the same shape. The same argument holds for d_{xy}. The description of these two orbitals in the above discussion in terms of cubic geometries is thus only an approximation.

Selection Rules

Transitions by dipole coupling between electronic energy states are subject to two selection rules: The spin must not change during the transition, and the transition must be between states of opposite parity (LaPorte's rule). Consider now the possible selection–rule relaxors—mechanisms which relax LaPorte's rule and allow at least some of the transitions to occur as weak absorptions.

P–orbital mixing and vibronic coupling are the two mechanisms most commonly involved. The mixing of the *d*–orbitals with higher *p*–orbitals can take place only if the transition metal is not on a centro–symmetric site. The transition probability for *p*–*d* mixing transitions is given by

$$P_{mn}{}^{(d-p)} \sim \int \psi_m \mu \psi_n \, d\tau$$

where μ is the dipole moment operator. P_{mn} can have a finite value only if the integral is totally symmetric with respect to the site group of the ion. The symmetry of the integral can be calculated by decomposing the direct product of the irreducible representation of the excited state in question, the component of the dipole moment (which transforms as x, y, or z) coupling the transition, and the ground state.[1]

[1] A very readable account of the use of group theory to determine selection rules may be found in Cotton (1971). For a more advanced discussion see Tinkham (1964).

Although x, y, and z are unique in any one 8–fold site, the other operations of the space group mix the labels between sites, so that there is no distinction when the full cubic unit cell is considered. There are effectively, then, only transitions of the type $A \rightarrow A$ and $A \rightarrow B$. All components of the dipole moment belong to representations of the B type. The products are:

$$A \times B \times A = B \text{ (antisymmetric)}$$
$$B \times B \times A = A \text{ (symmetric)}$$

Thus all of the $A \rightarrow B$ transitions are allowed, while the $A \rightarrow A$ transition in Figure 5 is forbidden by the mixing mechanism. The fact that the a–band is only a little less intense than the b– and c–bands and the fact that all molar extinction coefficients are low ($\epsilon \sim 1$), both suggest that orbital mixing is not effective. The mechanism is formally allowed by symmetry considerations, but the deviation of the 8–fold site from centro–symmetric symmetry is not sufficient to produce much coupling in a quantitative sense.

The selection rules for vibronic coupling are derived from

$$P_{mn}^{(\mathrm{vib})} \sim \int \psi_{em}{}^{*}\psi_{vm}{}^{*}\mu\psi_{en}\psi_{vn}\, d\tau$$

where ψ_{vm} is a vibrational excited state coupling the transition and ψ_{vn} is the vibrational ground state (always totally symmetric). Again the requirement for a finite transition probability is that the integral be totally symmetric. That is, the direct product of the representations of the five functions under the integral must belong to the A representation. Since the vibrational ground state is totally symmetric, it can be ignored and the selection rule reduces to the requirement that there exists a phonon mode whose symmetry is the same as the product representation of $\int \psi_{em}{}^{*}\mu\psi_{en}\, d\tau$. These products are the same as those calculated for the p–d mixing mechanism. Thus phonons of both A and B type are needed to account for all three spin–allowed bands.

The vibrational spectrum of the garnet structure has been examined theoretically by Hurrell *et al.* (1968) and by Moore, White, and Long (1971). There are 98 vibrational modes for the entire structure. However, it seems likely that only vibrations involving the cation on the 8–fold site would be effective in vibronic coupling. These are:

$$\Gamma(12c) = A_{2g} + A_{2u} + E_g + E_u + 3T_{1g} + 3T_{1u} + 2T_{2g} + 2T_{2u}.$$

The symmetry notation is that appropriate to the full factor group.

When reduced to the 8–fold site symmetry these modes become

$$\Gamma(D_2) = 6A + 10B_1 + 10B_2 + 10B_3.$$

Phonon modes occur in all D_2 representations, and so all transitions are formally allowed by vibronic coupling.

Vibronic coupling implies a particular dependence of the band intensities on temperature. Holmes and McClure (1957) proposed a dependence of the form

$$f = f_0(1 + e^{-\theta/T})$$

where f is the oscillator strength

$$f = 4.32 \times 10^{-9} \int \epsilon(\nu)\, d\nu$$

f_0 is the oscillator strength at 0 K and θ is the vibrational frequency of the coupling phonon in temperature units.

Oscillator strengths for the a, b, and c bands are plotted in Figure 7. The shapes of the curves are as expected for vibronic coupling, and they can fit to a function of the form

$$f = f_0(1 + \alpha e^{-\theta/T}).$$

The best–fit parameters are

	a	b	c
f_0	0.1×10^{-5}	0.1×10^{-5}	0.5×10^{-5}
α	68	146	14
θ	1200 K	1200 K	800 K
	(835 cm^{-1})	(835 cm^{-1})	(695 cm^{-1})

The vibrational frequencies are in reasonable agreement with observed infrared frequencies of 862 cm^{-1} and 630 cm^{-1} (Moore, *et al.*, 1971).

CRYSTAL CHEMICAL RELATIONS

Site Size and Site Distortion

If the mean of the Fe^{2+} frequencies is a measure of Dq in the 8–fold site, there should be an inverse relationship between the mean frequency and the mean metal oxygen distance. Four of the measured garnets, Al–77, Py–71, Sp–70, and Gr–90 were selected as being the most representative of the end member compositions. The mean

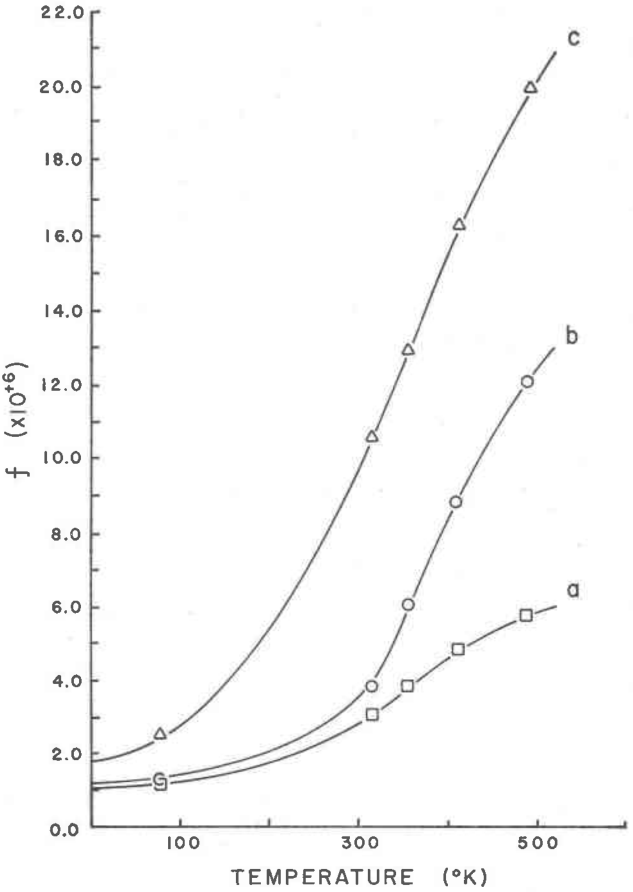

Fig. 7. Dependence of oscillator strength of spin-allowed bands on temperature.

of the three Fe^{2+} bands is plotted against $\langle X\text{–}O\rangle$ distances as reported by Novak and Gibbs (1971) in Figure 8. Although the total shift is small, only 450 cm^{-1}, and therefore difficult to measure from such broad bands, the result is as expected. Pyrope with the smallest site has the highest frequency and grossular with the largest site has the lowest frequency. An attempt to further refine the relationship by calculating a mean site size from weighted averages of Shannon–Prewitt (1969) ionic radii of the X–cations

$$\langle X\text{–}O\rangle = \sum_i N_{fi}(R_{xi} + R_0)$$

where N_{fi} is mole fraction of *ith* 8–fold cation and R_{xi} is its radius, and R_0 is 4-coordinated radius of O^{2-}, did not produce anything useful. The curve was similar to Figure 8, but the individual points were too scattered to calculate n in the crystal field relation

$$Dq \sim R_{x-0}^{-n}.$$

Variations in site distortion which produce unknown variations in the splitting of the ground state in addition to the limited precision possible in the measurements severely limit the calculation.

The assignments for the individual orbitals of Fe^{2+} in the 8-fold site place the d_{xz} orbitals along the short X–O bond and the d_{yz} orbital along the long X–O bond. It might be expected, therefore, that the separation in frequency between the c-band (assigned to d_{xz}) and the b-band (assigned to d_{yz}) would be a measure of the difference in X–O bond lengths and therefore a measure of the distortion of the 8-fold site. This frequency difference is plotted against the $\Delta(X\text{–O})$ values of Novak and Gibbs (1971) for the four definable end members in Figure 9. The relationship is very good within the limitations

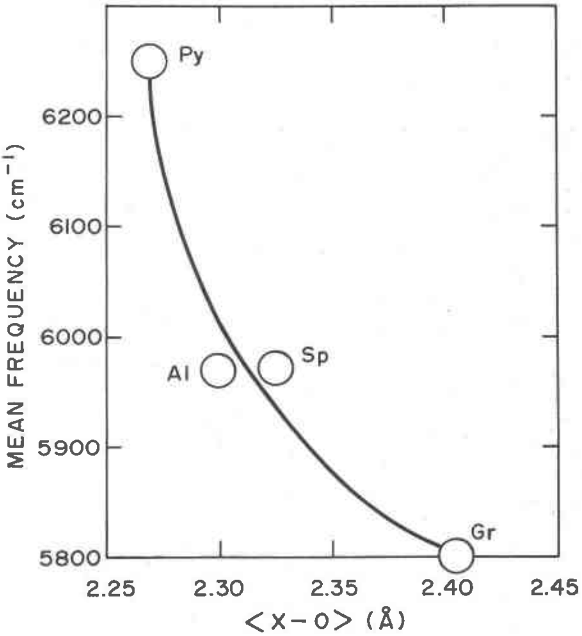

FIG. 8. Mean of T_{2g} orbital energies of Fe^{2+} as function of mean X–O distance. Frequencies of Py (pyrope), Al (almandine), and Sp (spessartite) are means of three observed bands. Frequency of Gr (grossular) is that of middle band, since low frequency band is not observed in this garnet.

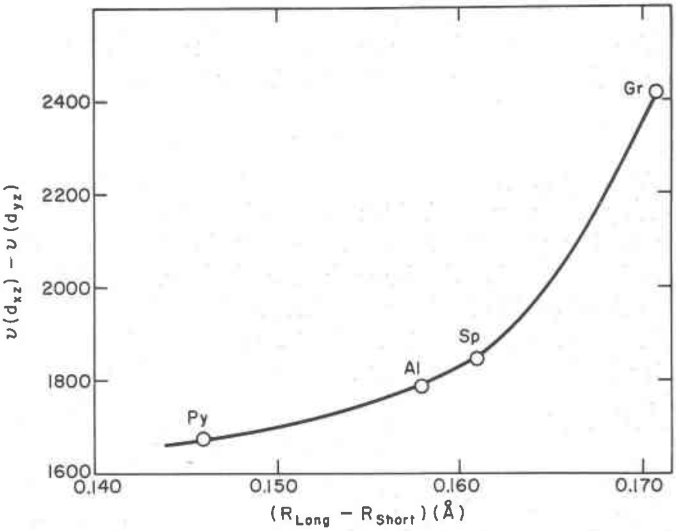

FIG. 9. The relation between the separation of the b– and c–bands and the distortion of the 8–fold site.

of the small number of points. The increased distortion of the dodecahedral site in grossular is very clearly reflected in the optical spectrum.

Crystal Field Stabilization Energies

The relative stability of transition ions in the 8–fold site of garnet and their partitioning between garnets and co–existing biotite was discussed by Schwarcz (1967). Burns (1970, p. 85) also made a calculation of the CFSE for Fe^{2+} in the 8–fold site of garnet. Burns apparently accepted Clark's (1957) 2900 cm^{-1} band (although he plots 3100 cm^{-1} on his energy level diagram) and assigned it to the upper component of the E_g ground state split by the D_2 distortion of the cubal field.[1] This assignment implies a large splitting of the cubic ground state which present data and assignments argue against and leads to a value of the CFSE of 4,160 cm^{-1} or 11.9 kcal.

Fe^{2+} has a single electron outside the half–filled shell. Placing this

---

[1] As noted earlier, neither we nor Manning were able to observe the 2900 cm^{-1} band, although Clark's figures show it to be quite intense. Clark's figures show spectra very similar to ours and Manning's, except for the numerical value of the lowest frequency band. Clark also reports a band at 2500 cm^{-1} in diopside, whereas all further measurements show this band to fall near 4500 cm^{-1} (See Burns, 1970, for summary of pyroxene spectra). We conclude that the low frequency bands reported by Clark suffer from a calibrational or calculational error and that the true value of these bands in pyrope, almandine, and diopside are about 2000 cm^{-1} higher than he reported.

electron in the lowest energy orbital (d_{z^2}) leads to an extra stabilization energy composed of a cubic field part and an additional part due to the ground state splitting. From Figure 5 it can be seen that

$$\mathrm{CFSE} = \frac{3}{5}\left[\left(\frac{\nu_a + \nu_b + \nu_c}{3}\right) - \frac{1}{2}\,(\text{ground state splitting})\right] + \frac{1}{2}\,(\text{ground state splitting})$$

The ground state splitting is unknown, but has been shown to be less than 1500 cm^{-1}. Ignoring this term will lead to CFSE's that are too small by a factor of one–fifth the E_g orbital splitting, or no more than 300 cm^{-1}.

The calculated CFSE's for the three end–member garnets for which all three bands can be measured are:

Py	3750 (cm^{-1})	10.72 kcal mole^{-1}
Al	3583	10.24
Sp	3588	10.26

These values are lower than those proposed by Burns because of the smaller contribution from the ground state splitting.

An examination of element partitioning in mineral assemblages such as the eclogites or schists where garnet co–exists with minerals with small divalent cations such as pyroxene or chlorite shows that the CFSE and ionic size effects work in opposite directions. The favorable CFSE in the smaller octahedral sites in pyroxene and olivine will tend to enrich those minerals in small cations with large CFSE such as Ni^{2+}. On the other hand, larger divalent cations such as Mn^{2+} (for which CFSE = 0 anyway) may be enriched in the garnet phase. Measurement of the element distribution between garnet and pyroxene and garnet and chlorite (Matsui and Banno, 1969/1970) shows the Ni^{2+} is highly depleted in garnet, while Co^{2+}, Fe^{2+}, and Mn^{2+} are enriched. The favorable CFSE of Co^{2+} and Fe^{2+} in the ferromagnesian minerals fails to overcome the size effect in garnet.

ACKNOWLEDGMENTS

This work was supported by the National Science Foundation under Grants GP 3232 and GA 29440.

REFERENCES

BLOOMFIELD, PHILIP, A. W. LAWSON, AND CHARLES REY (1961) Crystal field splitting and covalent bonding in Fe^{2+} silicate garnets. *J. Chem. Phys.* **34,** 749–756.

BURNS, ROGER G. (1969) Optical absorption in silicates. *In* S. K. Runcorn (ed.), *The Application of Modern Physics to the Earth and Planetary Interiors.* John Wiley and Sons, New York.

——— (1970) *Mineralogical Applications of Crystal Field Theory.* Cambridge University Press, Cambridge.

Clark, Sydney P. (1957) Absorption spectra of some silicates in the visible and near infrared. *Amer. Mineral.* **42**, 732–742.

Cotton, F. Albert (1971) *Chemical Applications of Group Theory, 2nd ed.*, John Wiley and Sons, New York.

Garner, C. D., and F. E. Mabbs (1970) Studies in eight coordination. Part I. Crystal field energies in the D_{2d} point group. *J. Chem. Soc.* **(A)**, 1711–1716.

Geller, S. (1967) Crystal chemistry of the garnets. *Z. Kristallogr.* **125**, 1–47.

Gibbs, G. V., and J. V. Smith (1965) Refinement of the crystal structure of synthetic pyrope. *Amer. Mineral.* **50**, 2023–2039.

Holmes, Owen G., and Donald S. McClure (1957) Optical spectra of hydrated ions of the transition metals. *J. Chem. Phys.* **26**, 1686–1694.

Hurrell, J. P., S. P. S. Porto, I. F. Chang, S. S. Mitra and R. P. Bauman (1968) Optical phonons of yttrium aluminum garnet. *Phys. Rev.* **173**, 851–856.

Jones, G. D. (1967) Jahn–Teller splittings in the optical absorption spectra of divalent iron compounds. *Phys. Rev.* **155**, 259–261.

Manning, P. G. (1967a) The optical absorption spectra of the garnets almandine-pyrope and spessartine and some structural interpretations of mineralogical significance. *Can. Mineral.* **9**, 237–251.

Manning, P. G. (1967b) The optical absorption spectra of some andradites and the identification of the $^6A_1 \rightarrow {}^4A_1\,{}^4E(G)$ transition in octahedrally bonded Fe^{3+}. *Can. J. Earth Sci.* **4**, 1039–1047.

Manning, P. G. (1969) Optical studies of grossular, andradite (var. colophonite) and uvarovite. *Can. Mineral.* **9**, 723–729.

Matsui, Yoshito, and Shohei Banno (1969/1970) Partition of divalent transition metals between coexisting ferromagnesian minerals. *Chem. Geol.* **5**, 259–265.

Moore, R. K., and W. B. White (1972) Electronic spectra of transition metal ions in silicate garnets. *Can. Mineral* (in press).

———, ———, and T. V. Long (1971) Vibrational spectra of the common silicates. I. The Garnets. *Amer. Mineral.* **56**, 54–71.

Novak, G. A., and G. V. Gibbs (1971) The crystal chemistry of the silicate garnets. *Amer. Mineral.* **56**, 791–825.

Prandl, Wolfram (1966) Verfeinerung der Kristallstruktur des Grossulars mit Neutronen–und Röntgenstrahlbeugung. *Z. Kristallogr.* **123**, 81–116.

Randić, Milan (1962) Ligand field splitting of *d* orbitals in eight coordinated complexes of dodecahedral structure. *J. Chem. Phys.* **36**, 2094–2097.

Schwarcz, Henry P. (1967) The effect of crystal field stabilization on the distribution of transition metals between metamorphic minerals. *Geochim. Cosmochim. Acta* **31**, 503–517.

Shannon, R. D., and C. T. Prewitt (1969) Effective ionic radii in oxides and fluorides. *Acta Crystallogr.* **B25**, 925–946.

Tinkham, Michael (1964) *Group Theory and Quantum Mechanics.* McGraw McGraw Hill Book Co., New York.

Wilson, E. G. Jr., J. C. Decius and P. C. Cross (1955) *Molecular Vibrations.* McGraw Hill Book Co., New York.

Manuscript received, May 10, 1972; accepted for publication, June 19, 1972.